

SOME TRANSITION METAL NITRATE COMPLEXES WITH HEXAMETHYLENETETRAMINE

Part LV. Preparation, X-ray crystallography and thermal decomposition

G. Singh^{1*}, B. P. Baranwal¹, I. P. S. Kapoor¹, D. Kumar¹, C. P. Singh¹ and R. Fröhlich²

¹Department of Chemistry, DDU Gorakhpur University, Gorakhpur 273009, India

²Organisch-Chemisches Institut, Universität Münster, 48149 Münster, Germany

Three hexamethylenetetramine (HMTA) metal nitrate complexes such as $[M(H_2O)_4(H_2O-HMTA)_2](NO_3)_2 \cdot 4H_2O$ (where $M=Co, Ni$ and Zn) have been prepared and characterized by X-ray crystallography. Their thermal decomposition have been studied by using dynamic, isothermal thermogravimetry (TG) and differential thermal analysis (DTA). Kinetics of thermal decomposition was undertaken by applying model-fitting as well as isoconversional methods. The possible pathways of thermolysis have also been proposed. Ignition delay measurements have been carried out to investigate the response of these complexes under condition of rapid heating.

Keywords: crystal structure, hexamethylenetetramine, ignition delay, iso-conversional, isothermal TG, metal nitrate, model fitting

Introduction

Nitrates are powerful oxidizing agents [1, 2] and decompose exothermically at elevated temperatures. Of the various classes of high energetic compounds (HECs), transition metal complexes find application in explosives, propellants and pyrotechnics. Moreover, transition metal complexes are potential burning rate modifier for HTPB-AP propellants [3, 4]. These transition metal complexes are used as precursor to obtain ultra fine metal oxides, which have interesting electrical, magnetic and catalytic properties [5]. Thermal analysis provides realistic information about the thermal stability of compounds. Recently, we have undertaken studies on the thermolysis and kinetics of some transition metal nitrate and perchlorate complexes with 1,4-diaminobutane [6, 7], propylenediamine [8, 9] ethylenediamine [4, 10] and 1,6-diaminohexane ligand [11].

Tetraazaadamantane, urotropine or commonly called hexamethylenetetramine (HMTA) in which four nitrogen atoms are situated at the corners of a tetrahedron, is a ligand of polycyclicpolydentate type. Its complexes in which HMTA acts as a monodentate ligand [12], bidentate ligand [13, 14] and shows non-chelating behaviour [15] (in low valent organometallic complexes). It is used for preparing RDX. Thus it was found interesting to prepare and characterize the transition metal nitrate complexes containing intermolecular hydrogen bonded hexamethylenetetramine. The thermolysis of these complexes has been done by TG and DTA techniques. The ignition delay of these samples has also been measured. Kinetics of thermolysis has been evaluated using both model fitting as well as isoconversional methods.

Experimental

Materials

The following chemicals were used as received; Cobalt carbonate, nickel carbonate (Thomas Baker), zinc carbonate, 70% HNO_3 (s.d.fine), hexamethylenetetramine (Lancaster) and silica gel TLC grade (Qualigens).

Preparation of the complexes

The hexahydrate metal nitrate complexes were obtained by treating metal carbonates with 70% nitric acid, washing the salts with petroleum ether, recrystallising from distilled water and dried over fused calcium chloride. The HMTA metal nitrate complexes were prepared by treating the aqueous solution of metal nitrate hexahydrates with aqueous solution of HMTA in appropriate stoichiometry.



where $M=Co, Ni$ and Zn , respectively.

The complexes were recrystallized from aqueous solutions and their purity was checked by thin layer chromatography (TLC). The complexes were characterized by X-ray crystallography.

Methods

X-ray crystallographic study

Crystals of the complexes were obtained by the recrystallisation from aqueous solutions. The data collection of the crystals were performed at low tem-

* Author for correspondence: gsingh4us@yahoo.com

perature (223 K) using a Nonius Kappa CCD diffractometer, equipped with a rotating anode generator Nonius FR591. Programs used: data collection Collect (Nonius B.V; 1998), data reduction and absorption correction Denzo-SMN [16]. The structures were solved by direct methods (SHELXS-97) [17] and refined by full-matrix least square method on all F^2 data using SHELXL-97 [18]. Hydrogen atoms were in part placed on calculated positions and refined riding, at the water molecules they were located from a difference Fourier map and refined independent. Refinement with anisotropic thermal parameters for non-hydrogen atoms led to the R -values of 0.036 (Co), 0.046 (Ni) and 0.033 (Zn). The crystal structures (graphics done with Schakal [19]) of the complexes are shown in Figs 1–3. The crystal parameters of the complexes are summarized in Table 1.

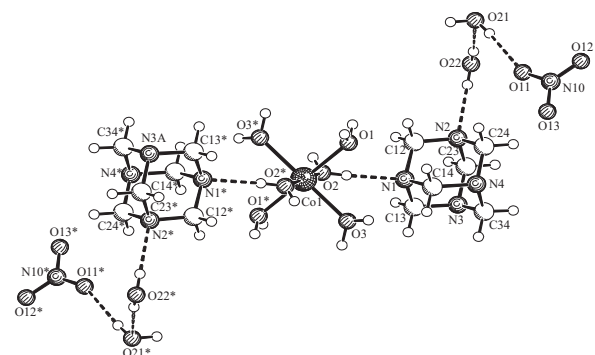


Fig. 1 Crystal structure of cobalt complex

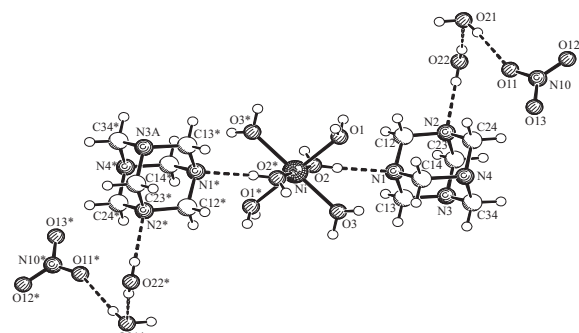


Fig. 2 Crystal structure of nickel complex

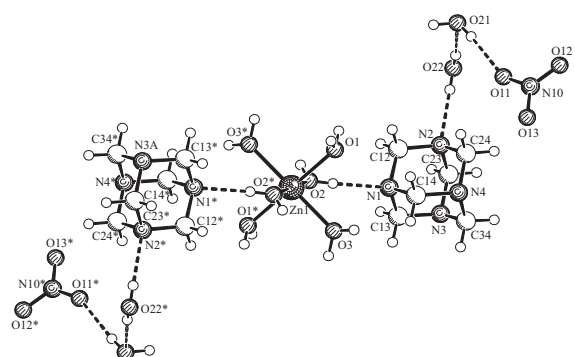


Fig. 3 Crystal structure of zinc complex

Experimental

Non-isothermal TG

TG studies on these complexes (mass 20 mg, 100–200 mesh) were undertaken in static air atmosphere at a heating rate of 5°C min⁻¹ using indigenously fabricated TG apparatus [20]. Gold crucible was used as sample holder. The curves of mass% vs. temperature (°C) are given in Fig. 4.

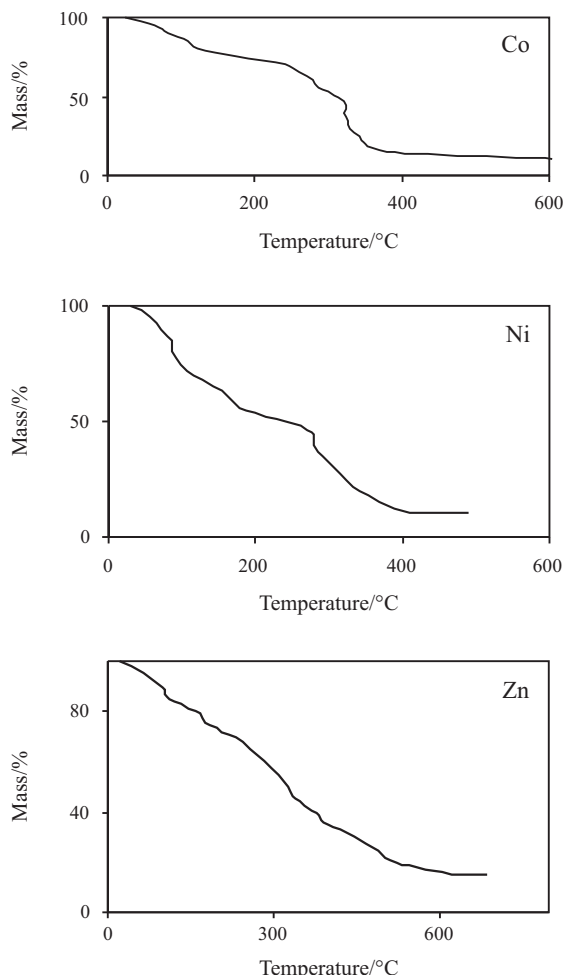


Fig. 4 Non-isothermal TG of complexes in air atmosphere

DTA curve of complexes were obtained on Universal Thermal Analyser Instrument, Mumbai, in static air (heating rate of 10°C min⁻¹). DTA curves of complexes are shown in Fig. 5. The TG and DTA phenomenological data are summarised in Table 2.

Isothermal TG

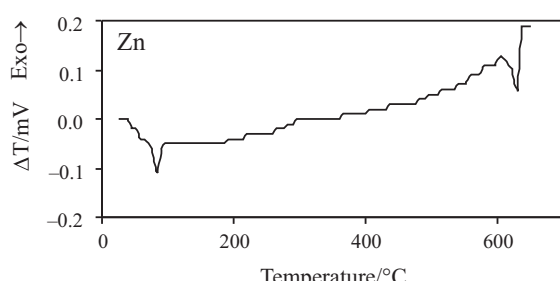
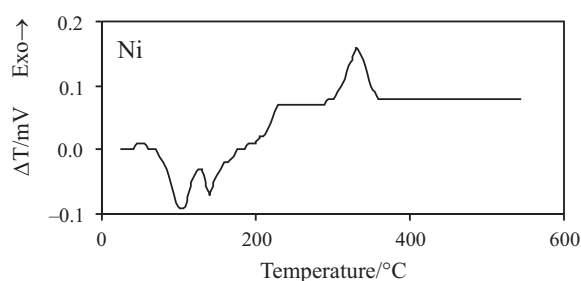
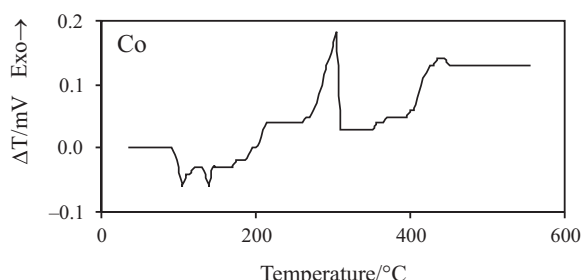
The isothermal TG on these complexes (mass 20 mg, 100–200 mesh) were carried out in static air atmosphere using above said TG apparatus [20] at appropriate temperatures and TG curves are presented in Fig. 6.

Table 1 Crystal and structure refinement data

Empirical formula	1 $C_{12}H_{44}CoN_{10}O_{16}$	2 $C_{12}H_{44}NiN_{10}O_{16}$	3 $C_{12}H_{44}N_{10}O_{16}Zn$
Colour	colorless	light green	Colorless
Formula mass	643.50	643.28	649.94
Temperature/K	223(2)	223(2)	223(2)
$\lambda/\text{\AA}$	0.71073	0.71073	0.71073
Crystal system	triclinic	triclinic	triclinic
Space group	P-1(No.2)	P-1(No.2)	P-1(No.2)
Cell constants	$a=9.023(1) \text{ \AA}, \alpha=88.29(1)^\circ$ $b=9.343(1) \text{ \AA}, \beta=75.70(1)^\circ$ $c=9.653(1) \text{ \AA}, \gamma=61.78(1)^\circ$	$a=8.993(1) \text{ \AA}, \alpha=87.72(1)^\circ$ $b=9.265(1) \text{ \AA}, \beta=75.73(1)^\circ$ $c=9.667(1) \text{ \AA}, \gamma=61.38(1)^\circ$	$a=9.019(1) \text{ \AA}, \alpha=88.03(1)^\circ$ $b=9.323(1) \text{ \AA}, \beta=75.61(1)^\circ$ $c=9.687(1) \text{ \AA}, \gamma=61.63(1)^\circ$
Volume	691.21(13) \AA^3	682.32(13) \AA^3	690.86(13) \AA^3
Molecules per unit cell, Z	1	1	1
Calculated density	1.546 Mg m^{-3}	1.562 Mg m^{-3}	1.562 Mg m^{-3}
Absorption coefficient	0.708 mm^{-1}	0.799 mm^{-1}	0.976 mm^{-1}
$F(000)$	341	342	344
Crystal size/mm	0.35×0.25×0.15	0.40×0.30×0.20	0.40×0.25×0.20
θ range for data collection	2.19 to 28.01°	2.18 to 27.74°	2.18 to 28.52°
Limiting indices	-11≤ h ≤11, -12≤ k ≤10, -12≤ l ≤8	-11≤ h ≤11, -12≤ k ≤11, -11≤ l ≤12	-11≤ h ≤12, -10≤ k ≤12, -12≤ l ≤12
Reflections collected/unique	6349/3179 [$R(\text{int})=0.051$]	7580/3009 [$R(\text{int})=0.054$]	7998/3387 [$R(\text{int})=0.040$]
Reflections observed [$I>2\sigma(I)$]	2770	2612	3068
Data/restraints/parameters	3179/0/219	3009/0/219	3387/0/219
Goodness-of-fit on F^2	1.058	1.056	1.057
Final R indices [$I>2\sigma(I)$]	$R_I=0.036, wR^2=0.089$	$R_I=0.046, wR^2=0.120$	$R_I=0.033, wR^2=0.084$
R indices (all data)	$R_I=0.044, wR^2=0.094$	$R_I=0.055, wR^2=0.127$	$R_I=0.039, wR^2=0.088$
Extinction coefficient	0.030(6)	0.043(14)	0.044(6)
Largest diff. peak and hole/e \AA^{-3}	0.39 and -0.61	0.41 and -0.55	0.39 and -0.44
CCDC number	639634	639635	639636

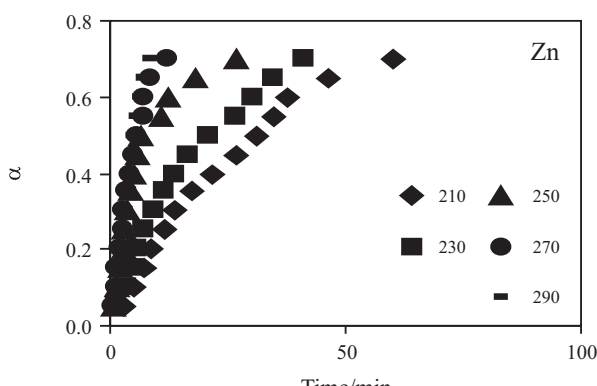
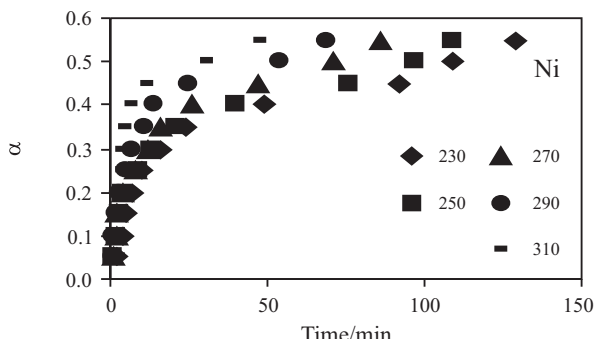
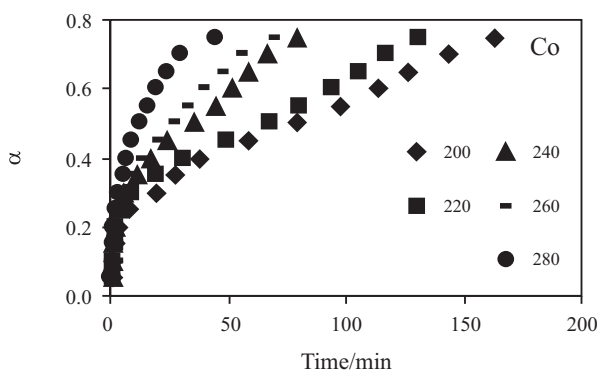
Table 2 TG-DTA phenomenological data of the complexes under air atmosphere

Complex	Step	TG		DTA	
		$T_{\text{range}}/^{\circ}\text{C}$	decomposition/%	peak temp./ $^{\circ}\text{C}$	nature
1	I	93–100	11.2	95	endo
	II	132–140	11.2	140	endo
	III	290–315	65.6	305	exo
2	I	95–110	11.2	105	endo
	II	120–145	11.2	140	endo
	III	320–340	65.0	330	exo
3	I	65–100	11.0	85	endo
	II	600–645	76.0	630	endo

**Fig. 5** DTA curve of complexes in air atmosphere

Ignition delay (D_i) measurements

These studies were undertaken using tube furnace (TF) technique [21]. 20 mg samples (100–200 mesh) were taken in an ignition tube (l~5 cm, d~0.5 cm) and time interval between the insertion of the ignition tube into the TF and the moment of ignition indicated by the appearance of fumes with light and noise noted with help of stop watch, gave the value of ignition delay in seconds. The sample was inserted into the TF with the help of a bent wire. The time for the insertion of the ignition tube into the TF was kept constant

**Fig. 6** Isothermal TG of complexes

throughout each run. The accuracy of temperature measurements of TF was $\pm 1^{\circ}\text{C}$. Each run was taken five times and mean D_i value are reported in Table 3.

Table 3 Ignition delay activation energy for thermal ignition (E^*) and correlation coefficient (r) for the complexes

Complex	D_i/s at temperature/ $^\circ\text{C}$					$E^*/\text{kJ mol}^{-1}$	r
	280±1	300±1	320±1	340±1	360±1		
1	85	68	61	50	40	27.5	0.9984
2	107	90	85	60	45	27.7	0.9953
3	72	63	57	48	39	23.8	0.9997

Kinetic analysis

Isothermal TG data taken at appropriate temperatures have been used to evaluate the kinetics of early thermolysis. Kinetics is evaluated by using the model fitting [22] as well as isoconversional method by Vyazovkin and Wight [23]. The following equation is found to hold under isothermal condition

$$-\ln t_{\alpha,i} = \ln[A/g(\alpha)] - E_\alpha/RT_i \quad (1)$$

where α is the extent of conversion, E_α is the activation of energy at a particular α , R the gas constant and T_i the absolute temperature. Thus, the values of E_α were evaluated at various α_i . The dependencies of E_α on extent of conversion are presented in Fig. 8.

The kinetics of fast decomposition is evaluated from the ignition delay (D_i). The D_i data were found to fit in the following equation [21, 24]

$$D_i = Ae^{E^*/RT} \quad (2)$$

where E^* is the activation energy for ignition, A the Arrhenius factor and T is the absolute temperature. The values of E^* were obtained from the slope of $\ln D_i$ vs. $1/T$ (Fig. 7).

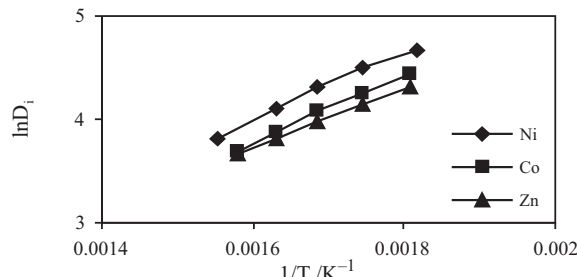


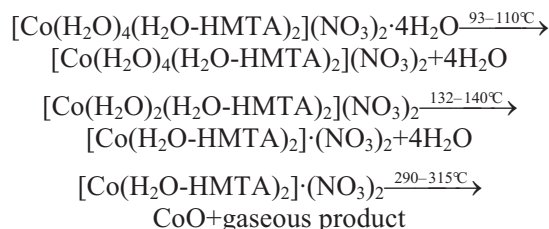
Fig. 7 Plot of $\ln D_i$ vs. $1/T$ for the elements shown

Results and discussion

The crystal structures of the complexes are shown in Figs 1–3. The two HMTA molecules are attached with the metal ion through water molecules. The bonding between the HMTA and the water is clearly shown to be hydrogen bonding. Each HMTA is attached by two hydrogen bonds between nitrogen of HMTA and hydrogen of the water. The nitrate ion is also attached to the water molecule via hydrogen bonding. Therefore the molecular formula of a single crystal can be repre-

sented as $[M(H_2O)_4(H_2O-HMTA)_2](NO_3)_2 \cdot 4H_2O$, where $M=(\text{Co, Ni or Zn})$, which is matched with the empirical formula of the compound given in the text.

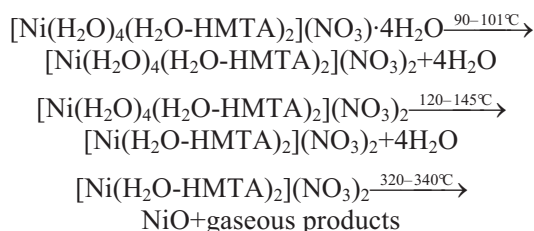
It is evident that all these complexes undergo decomposition for involving more than one step, to give metal oxide as residue and other various gaseous decomposition products (Fig. 4). TG curve for the cobalt complex shows that it decomposes in the three steps in static air. Corresponding to these, three DTA peaks are obtained (Fig. 5). In the first step (93–100°C) four of the water molecules leave (~11.2% mass loss). In the next second step (132–140°C) four water molecules are coordinated with the metal leave (~11.2% mass loss). In the third step (290–315°C), water, HMTA molecules decomposes (~65.60% mass loss) and a residue (~12%) of cobalt oxide is left. Thus the mechanistic pathways of thermolysis of the cobalt complex may be proposed as:



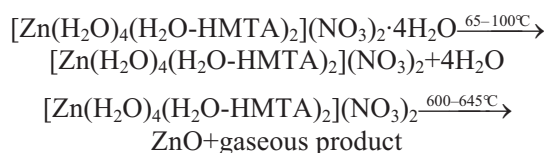
An endothermic peak at 95°C in DTA curves, is obtained for the removal of four water molecules. For the second step one sharp endotherm is obtained due to removal of four water molecules coordinated with metal. An exotherm is obtained at 305°C which is due to exothermic decomposition of the dehydrated complex.

Nickel complex decomposes in three steps (Fig. 4). The first step (95–110°C) is due to loss of four water molecules (~11.2% mass loss) giving one endothermic peak at 105°C in DTA. This endotherm is due to removal of four water molecules. In the second step of the decomposition (120–145°C), four water molecules which are coordinated to the metal, leave (~11.2% mass loss). Corresponding to this decomposition step an endotherm at 140°C in DTA was obtained. In the third step, the dehydrated complex decomposes between 320–340°C (~65% mass loss) giving nickel oxide as residue and an endotherm at 330°C in DTA (Fig. 5). This exotherm in DTA is due to exothermic decomposition of ni-

trate ion from the dehydrated complex. Thus the pathways for the thermolysis of nickel complex may be proposed as:



Zn complex decomposes in two steps in static air atmosphere. In the first step ($65-100^\circ\text{C}$), four water molecules leave the complex (~11% mass loss) giving an endotherm at 85°C in DTA (Fig. 5). In the second step ($600-645^\circ\text{C}$), the dehydrated complex decomposes endothermically (~76% mass loss). An endotherm is also obtained in DTA curve at $\sim 630^\circ\text{C}$ (Fig. 5). Zinc oxide was ultimately obtained and the proposed pathways for the decomposition of zinc complex may be given as:



Similar pathways have been suggested for the thermal decomposition of nitrate and perchlorate complexes of transition metals with 1,4-diaminobutane, propylenediamine, ethylenediamine and nitrate complexes of 1,6-diaminohexane ligands [5–11]. In the present case, there is no indication for the formation of mono ligand intermediate. This may be attributed to the polycyclic chain of the HMTA molecules.

The kinetic analysis applying model fitting approach using isothermal TG data, gives an average activation energy 39.3, 31.05 and 63.6 kJ mol^{-1} upto $\alpha=0.75$, 0.55 and 0.70, respectively. The isothermal TG data shows that the solid-state decomposition of these complexes is not as simple as indicated by the

model fitting method. The value of activation energy varies with extent of conversion (α) (Fig. 8). The value of E for Zn complex is higher than that of Ni and Co complex. Except in higher α range, E for Ni is greater than Co indicating the greater stability of Ni complex over Co complex.

All these complexes are quite stable at room temperature but they ignite with noise, light and fume on sudden high heating. Ignition delay data (Table 3) shows that time for ignition at a fixed temperature is in the order Ni>Co>Zn. This shows that Ni complex is more stable than Co because of higher nuclear charge. Zn complex is less stable due to completely filled valence shell d -orbital.

Conclusions

HMTA is coordinated with water molecule through hydrogen bonding. The nitrate ion is also attached to HMTA through water. The thermal stability of the complexes was found in the order Ni>Co>Zn by ignition delay.

References

- B. T. Encyclopedia of Explosives and related Items, Vol. 1, Picatinny Arsenal, New Jersey.
- J. H. Koper, O. G. Jansen and P. J. Vanden, Berg. Explosive Stoff, 8 (1970) 181.
- G. Singh, I. P. S. Kapoor and D. K. Pandey, J. Energ. Mater., 20 (2002) 223.
- G. Singh and D. K. Pandey, Propellants, Explos. Pyro., 28 (2003) 5.
- S. Y. Sawant, K. R. Kannan and V. M. S. Verneker, 13th National Symposium on Thermal Analysis BARC, Mumbai, India 2002.
- G. Singh, C. P. Singh and S. M. Mannan, J. Hazard. Mater., 122 (2005) 111.
- G. Singh, C. P. Singh and S. M. Mannan, Thermochim. Acta, 437 (2005) 21.
- G. Singh and D. K. Pandey, Combust. Flame, 135 (2003) 135.
- G. Singh and D. K. Pandey, J. Therm. Anal. Cal., 82 (2005) 353.
- G. Singh, S. Prem Felix and D. K. Pandey, Thermochim. Acta, 411 (2004) 61.
- G. Singh, C. P. Singh and S. M. Mannan, J. Hazard. Mater., A135 (2006) 10.
- W. Strohmeier and J. F. Guttenberger, Chem. Ber., 96 (1963) 2112.
- I. S. Ahuja, C. L. Yadava and S. Tripathi, Ind. J. Chem., (1989) 167.
- I. S. Ahuja and S. Tripathi, Chemistry Education, October–December 1990.
- A. Luttinghaus and W. Kullick, Tetrahedron Lett., 10 (1959) 13.

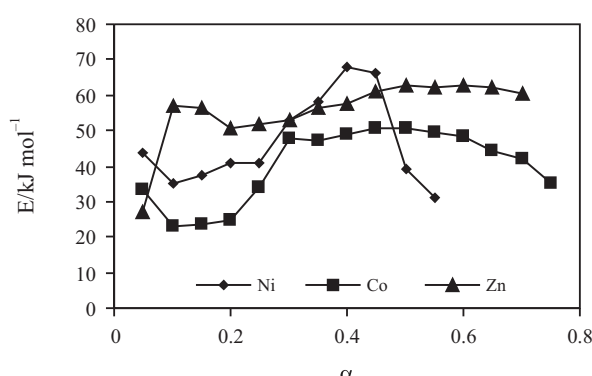


Fig. 8 Dependence of activation energy (E) on the extent of conversion (α) for the complexes of the elements shown

- 16 Z. Otwinowski and W. Minor, Methods Enzymol., 276 (1997) 307.
- 17 G. M. Sheldrick, Acta Cryst. A, 46 (1990) 467.
- 18 G. M. Sheldrick, SHELXL-97, Program for Crystal Structure Refinement, University of Gottingen, Germany 1997.
- 19 E. Keller, SCHAKAL, A computer program for the graphic representation of molecular and crystallographic models, University of Freiburg, Germany 1997.
- 20 G. Singh and R. R. Singh, Res. Ind., 23 (1978) 92.
- 21 G. Singh, I. P. S. Kapoor and S. K. Vasudeva, Ind. J. Technol., 29 (1991) 589.
- 22 S. Vyazovkin and C. A. Wight, J. Phys. Chem., A101 (1997) 8279.
- 23 N. Semenov, Chemical Reactions, Clarendon Press, Oxford 1935, Chapter 18.
- 24 E. S. Freeman and S. Gorden, J. Phys. Chem., 60 (1956) 867.

Received: July 4, 2007

Accepted: July 30, 2007

DOI: 10.1007/s10973-007-8615-5